

TOWSON UNIVERSITY

OFFICE OF GRADUATE STUDIES

**THE OPTICAL PROPERTIES OF A FERROFLUID IN APPLIED MAGNETIC
FIELD: HYPERBOLIC METAMATERIAL**

by

Bradley J. Yost

A thesis presented to the faculty of Towson University in partial fulfillment of the
requirements for the degree of Master of Science

Department of Physics, Astronomy, and Geosciences

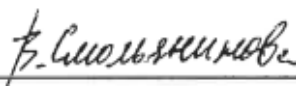
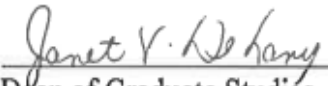
Towson University

Towson, MD 21252

May, 2014

**TOWSON UNIVERSITY
OFFICE OF GRADUATE STUDIES
THESIS APPROVAL PAGE**

This is to certify that the thesis prepared by Bradley J. Yost
entitled [INSERT Title of Thesis] The Optical Properties of a Ferrofluid in Applied
Magnetic Field: Hyperbolic Metamaterial
has been approved by the thesis committee as satisfactorily completing the thesis
requirements for the degree Master of Science
(for example, Master of Science)

<u>Dr. Vera Smolyaninova</u> Chair, Thesis Committee		<u>04.30.2014</u> Date
<u>Dr. Jeff Simpson</u> Committee Member		<u>2014 April 30</u> Date
<u>Dr. Phuoc Ha</u> Committee Member		<u>04.30.2014</u> Date
<u>Janet V. DeLong</u> Dean of Graduate Studies		<u>May 1, 2014</u> Date

Acknowledgements

I would like to thank the thesis committee, Dr. Jeff Simpson and Dr. Phuoc Ha, for taking time out of their busy schedules to be on the committee. I would like to thank Dr. Vera Smolyaninova for giving me the opportunity to be part of her research and for being the chair of the thesis committee. I would also like to thank Dr. Igor Smolyaninov for his assistance with the experiments and his help in understanding some of the theory behind the experiments. I would also like to thank Jeff Klupt and Bob Kuta for their assistance in building certain components of the experiments.

Abstract

The Optical Properties of a Ferrofluid in Applied Magnetic Field: Hyperbolic Metamaterial

Bradley J. Yost

In this study we examine the optical properties of a cobalt based ferrofluid when a magnetic field is applied. By performing optical transmission measurements we show that when a strong enough magnetic field is applied the ferrofluid behaves as a hyperbolic metamaterial. A hyperbolic metamaterial is a material that has unique optical properties which cause it to behave as a metal for one polarization direction of light and as a dielectric for the orthogonal polarization direction. By performing Fourier Transform Infrared (FTIR) spectroscopy we further demonstrate the unique properties of ferrofluid as hyperbolic metamaterial such as extreme sensitivity of the material to monolayer coatings of cobalt nanoparticles, which is relevant to applications in biological and chemical sensing. We also show that the ferrofluid can be used as a Minkowski spacetime analogue, where thermal fluctuations in our ferrofluid look similar to the creation and disappearance of individual Minkowski spacetimes.

Table of Contents

List of Figures	vii
Introduction	1
Metamaterials	1
Hyperbolic Metamaterials	2
Ferrofluids	5
Application of the Maxwell-Garnett Approximation to Hyperbolic Metamaterials	6
Experimental Methods	7
Transmission of light through the ferrofluid	8
Real time microscopic evaluation of ferrofluid	9
Fourier Transform Infrared (FTIR) spectroscopy of the ferrofluid	10
Experimental Results and Discussion	12
Application of Maxwell-Garnett approximation to Co-based Ferrofluid	13
Hyperbolic metamaterial as Minkowski Spacetime analogue	18
Thermal fluctuations of the nanoparticle volume fraction in ferrofluids	18

Hyperbolic metamaterials as Minkowski spacetime analogue	20
Polarization “notch”	22
FTIR spectroscopy	24
Conclusions	26
Bibliography	28
Curriculum Vita	31

List of Figures

Figure 1: Metamaterial designed by Shelby et al	1
Figure 2: Surfaces of constant frequency	4
Figure 3: Typical structures of hyperbolic metamaterials	4
Figure 4: Schematic representation of the ferrofluid	5
Figure 5: Cryo-TEM images	6
Figure 6: Schematic of transmission experiment	8
Figure 7: Setup for image capture	9
Figure 8: Block diagram of FTIR spectrometer	10
Figure 9: Setup used inside FTIR	11
Figure 10: Real time observation of the ferrofluid	12
Figure 11: Optical properties of cobalt	13

Figure 12: Wavelength dependencies of $\epsilon_{x,y,z}$	14
Figure 13: α_H plotted versus free space wavelength of light	15
Figure 14: FTIR spectroscopy data	15
Figure 15: Experimentally measured transmission of the cobalt based ferrofluid	16
Figure 16: Transmission data for different wavelengths	17
Figure 17: Experimentally observed thermal fluctuations	21
Figure 18: Fluctuations for different nanoparticle concentrations	22
Figure 19: Polarization and magnetic field dependence of ferrofluid transmission	23
Figure 20: FTIR transmission of the diluted ferrofluid	25
Figure 21: FTIR reflection of the non-diluted ferrofluid	26

Chapter 1

Introduction

1.1 Metamaterials

Metamaterials are materials that are engineered to have properties that are not normally found in nature. These properties include the ability of a metamaterial to behave as a dielectric for light with one polarization direction, and a metal for light with the opposite polarization direction. Metamaterials are extremely difficult to make; often requiring a structure to be created that is on the subwavelength scale, and can generally only be made as a 2 dimensional material. In 2000, Shelby et al [1] created a metamaterial from a series of split ring resonators using a shadow mask/etching technique. Fig. 1 is the schematic that demonstrates their metamaterial.

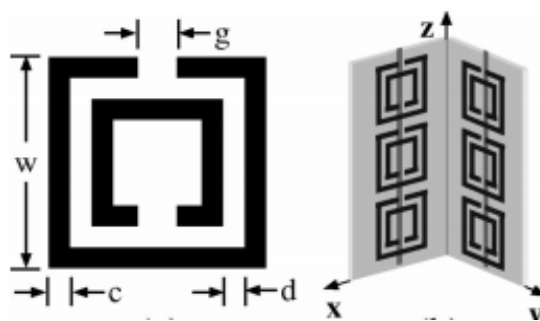


Fig. 1. Metamaterial designed by Shelby et al [1]

The split ring resonators were aligned with a wire through them so that six of the resonators were grouped together. The printed circuit board material that was used was 0.25 mm fiberglass, and the resonators and the wire strips were 0.03 mm copper; this metamaterial works in the microwave range, $f = 10 \text{ GHz}$ ($\lambda = 0.03 \text{ m}$). To extend this

metamaterial to the infrared (IR) and visible range would be very difficult, because the unit cell of the metamaterial should be several times smaller than the wavelength of light.

1.2 Hyperbolic Metamaterials

A subcategory of metamaterials are hyperbolic metamaterials, these metamaterials are fascinating because they allow wave vectors (k) to be infinitely large. This is allowed because of unusual anisotropic dispersion relation of hyperbolic metamaterial.

The dispersion of isotropic materials is given by

$$\frac{k_x^2 + k_y^2 + k_z^2}{\epsilon} = \frac{\omega^2}{c^2} \quad (1)$$

where ϵ is the dielectric function and ω is the frequency of the electromagnetic wave. In this study we use CGS units making ϵ dimensionless. For anisotropic materials the dispersion relation can be written as a sum of the dispersion relations along different axes:

$$\frac{k_z^2}{\epsilon_{zz}} + \frac{k_y^2}{\epsilon_{yy}} + \frac{k_x^2}{\epsilon_{xx}} = \frac{\omega^2}{c^2} \quad (2)$$

Where k represents the wave vector and ϵ represents the dielectric tensor for the indicated direction. When Eqn. 2 is used to describe a material, the material is said to be an elliptical material, this is because when Eqn. 2 is plotted, the graph is that of a 3D ellipsoid (Fig. 2a), and the surface of this ellipsoid describes the values that are allowed for the k -vector for a given frequency. Note that for metals below plasma frequency the real part of dielectric function is negative and that is why light will not propagate through

a metal. If one (or two) of the components of the dielectric tensor is negative, the resulting plot will be a hyperboloid, which extends out to infinity.

$$\frac{k_z^2}{\epsilon_{zz}} - \frac{k_y^2}{\epsilon_{yy}} - \frac{k_x^2}{\epsilon_{xx}} = \frac{\omega^2}{c^2} \quad (3)$$

Eqn. 3 represents a hyperbolic dispersion relation plotted in Fig. 2b. Just like the surface of the ellipsoid represents all of the allowed wave vector values for anisotropic materials, the surface of the hyperboloid represents all of the allowed wave vector values for the hyperbolic metamaterial. Fig. 2b shows that there is no limitation on k-vector in hyperbolic metamaterials.

Another peculiarity of hyperbolic metamaterial is infinite photonic density of states (PDOS). The PDOS is given by [2]

$$D(\omega)d\omega \propto \int_{shell} d^3k, \quad (4)$$

where the integral is extended over the volume of the shell in k space bounded by two surfaces on which the photon frequency is constant, one surface on which the frequency is ω and the other on which the frequency is $\omega+d\omega$ (Fig. 2c). Therefore, the ellipsoid, with its finite volume of such shell, has a finite density of states (Fig. 2c). But, the hyperboloid extends toward infinity, thus it has an infinite volume of such shell. This means that the hyperbolic metamaterial can support an infinite PDOS.

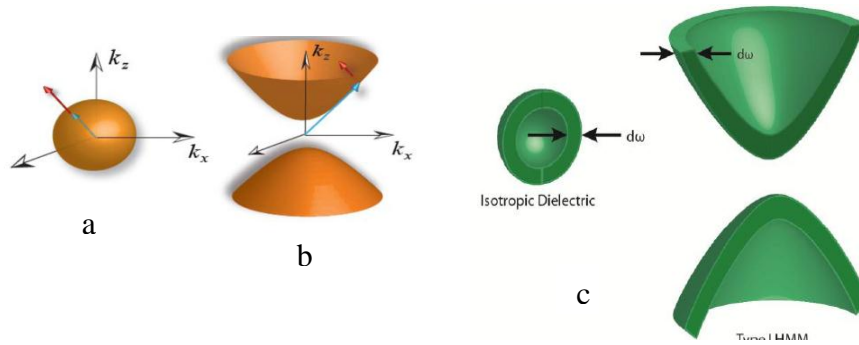


Fig. 2. Surfaces of constant frequency for (a) elliptical material and (b) hyperbolic metamaterial described by Eqn. 3. (c) The shell in k space bounded by two surfaces on which the photon frequency is constant, one surface on which the frequency is ω and the other on which the frequency is $\omega+d\omega$ for elliptical material (left) and hyperbolic metamaterial (right) [3]

It has been shown [4,5] that because of the PDOS of hyperbolic metamaterials there is an increase of the radiative decay rate for dye molecules that are on top of a hyperbolic metamaterial substrate. Narimanov et al [6] have further shown that reduced reflection is present in hyperbolic metamaterials because of the PDOS.

Hyperbolic metamaterials can be made in various ways, the two most common are by layering or stacking alternating metals and dielectrics in a process similar to thin film growth, or by embedding arrays of parallel metallic nanowires into a dielectric matrix.

Fig. 3 shows these common structures of hyperbolic metamaterials.

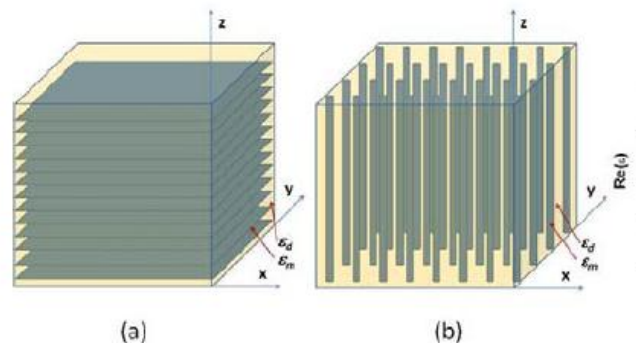


Fig. 3. Typical structures of hyperbolic metamaterials: (a) layered metal-dielectric metamaterial; (b) wire grid array.

1.3 Ferrofluids

Hyperbolic metamaterial structures are very difficult to make, however it is known that ferrofluids can form nanocolumns when a magnetic field is applied [7, 8, 9], which suggests a possibility to use a ferrofluid as a hyperbolic metamaterial. Ferrofluids are colloidal suspensions of nanoscale (<10 nm) ferromagnetic particles in a carrier fluid. Each particle is coated with a surfactant which inhibits clumping. This coating causes the magnetic attraction of the nanoparticles to become weak enough so that no particle agglomeration occurs in the absence of a magnetic field (Fig/ 4a). When a magnetic field is applied, the ferromagnetic particles form into nanocolumns, which are aligned to the direction of the magnetic field (Fig. 4b). When the magnetic field is applied, the ferrofluid will have a similar structure to 3b, with a column diameter of approximately the same size (10 nm) of the nanoparticles. Fig. 5 shows cryo-TEM images of a Fe_3O_4 ferrofluid forming into nanocolumns when a magnetic field is applied as described by Butter et al [9].

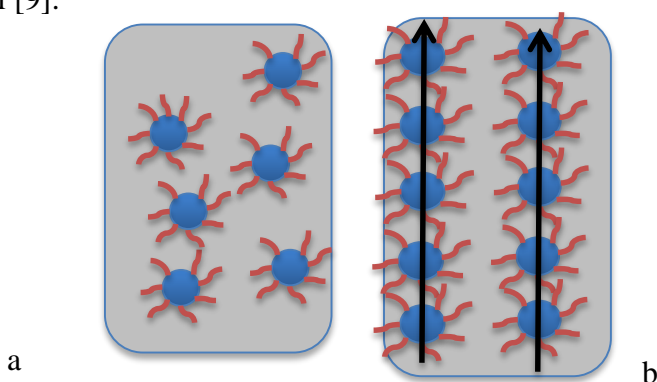


Fig. 4. Schematic representation of the ferrofluid. The blue circles are the ferromagnetic particles, the red lines represent the surfactant, and the grey background represents the carrier fluid. (a) When no magnetic field is applied, the nanoparticles are in random order; (b) When a magnetic field is applied, the nanoparticles align into nanocolumns. The black arrows represent the magnetic field lines.

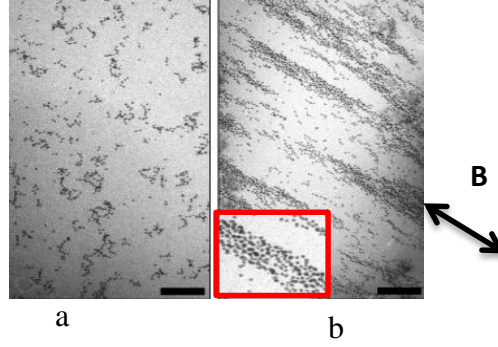


Fig. 5. Cryo-TEM images as described in [9]: (a) no magnetic field applied; (b) chains of particles oriented along the magnetic field indicated by the arrow; the inset is a 4x enlargement of one part of the image. The scale bars are 200nm.

1.4 Application of the Maxwell-Garnett Approximation to Hyperbolic Metamaterials

The Maxwell-Garnett Theory describes the bulk effective permittivity of a composite media in terms of the permittivity of the inclusion and the host dielectric constant. For a metal-dielectric composite medium, the metal can be considered the inclusion, and the dielectric can be considered the host [10]. The Maxwell-Garnett Approximation can be used to better understand the electromagnetic properties of our ferrofluid system. For our study we used a cobalt based ferrofluid, which was chosen because of the dielectric constants of kerosene ($\epsilon_d = 1.93$) and cobalt ($Re\epsilon_m = -9.0$) at 1500 nm. We apply the Maxwell-Garnett approximation [11] to calculate the components of the dielectric tensor for the ferrofluid in magnetic field:

$$\epsilon_z = n\epsilon_m + (1 - n)\epsilon_d \quad (5)$$

$$\epsilon_{x,y} = \frac{2n\epsilon_m\epsilon_d + (1-n)\epsilon_d(\epsilon_d + \epsilon_m)}{(1-n)(\epsilon_d + \epsilon_m) + 2n\epsilon_d} \quad (6)$$

where n is the average volume fraction of the ferromagnetic nanoparticle phase, and ϵ_m and ϵ_d are the dielectric permittivities of the ferromagnetic and liquid phase respectively. The most interesting situations arise when $\epsilon_m < 0$, which correspond to ferromagnetic particles being metallic or being coated with metal. In these situations the ferrofluid becomes a hyperbolic metamaterial if

$$n > n_H = \frac{\epsilon_d}{\epsilon_d - \epsilon_m} \quad (7)$$

At this concentration, ϵ_2 changes sign from positive to negative, while ϵ_1 remains positive if $-\epsilon_m \gg \epsilon_d$.

Chapter 2

Experimental Method

To study optical properties of ferrofluids three different experimental methods were used. First, transmission as a function of polarization and magnetic field was measured for different discrete wavelengths of light. Second, real time microscopic images of ferrofluid were studied with and without magnetic field for different wavelengths. Finally, FTIR spectroscopy was performed to see how broadband transmission of light was affected. In our experiments we used cobalt magnetic fluid 27-0001 from Strem Chemicals composed of 10 nm cobalt nanoparticles in kerosene with AOT (sodium dioctylsulfosuccinate) and LP4 (a fatty acid condensation polymer). This fluid was chosen because of the dielectric constants of kerosene ($\epsilon_d=1.93$) and cobalt ($Re\epsilon_m = -9.0$) at 1500 nm.

2.1 Transmission of light through the ferrofluid

Fig. 6 shows the schematic of our experimental setup. The laser light passes through a quarter wave plate to change the linearly polarized light to circularly polarized light. This is done so that the polarization dependence of the transmitted light can be measured. The ferrofluid is placed between two coils carrying current to create a uniform magnetic field. The light then passes through a polarizer then through a chopper for reference and to the detector where the intensity is measured using a lock-in amplifier technique.

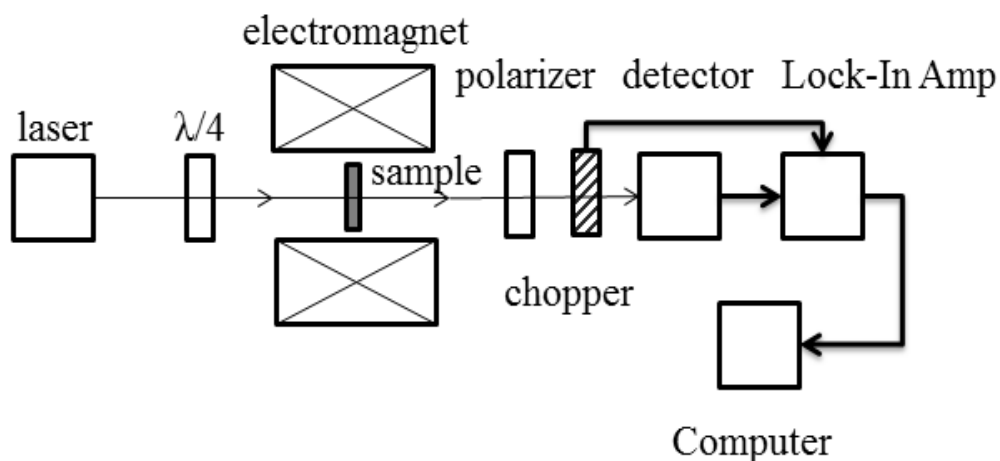


Fig. 6. Schematic of transmission experiment

In this experiment the strength of the magnetic field is steadily increased by increasing the current through the coils and the intensity of the laser is measured for different polarization angles. The strength of the magnetic field was measured using a F.W. Bell Gaussmeter. The magnetic field at the center of the coils was measured as a function of current in the coils and later used as calibration. The highest magnetic field strength that could be obtained with the coils was 300 G. For higher magnetic field strength a permanent magnet was used. The strength of magnetic field produced by the permanent

magnet at the position of the sample was measured with the Gaussmeter. For the transmission experiment the ferrofluid was placed in a quartz cell that had a volume of $4\mu\text{L}$, and a path length of $10\mu\text{m}$.

2.2 Real time microscopic observation of ferrofluid

To further understand the behavior of the ferrofluid when a magnetic field was applied, real time microscopic observation of ferrofluid was undertaken. In order to do this, we put the ferrofluid under a microscope and transmitted the laser light through the sample. The laser light was directed using a 45° dielectric mirror. 1550 nm wavelength laser light with fixed power and 4.5mW power, and 488 nm wavelengths laser light of variable power up to 50 mW power and corresponding cameras were used to capture the videos, using a camera attachment to the microscope that would record images. Fig. 7 shows the setup and schematic for the experiment.

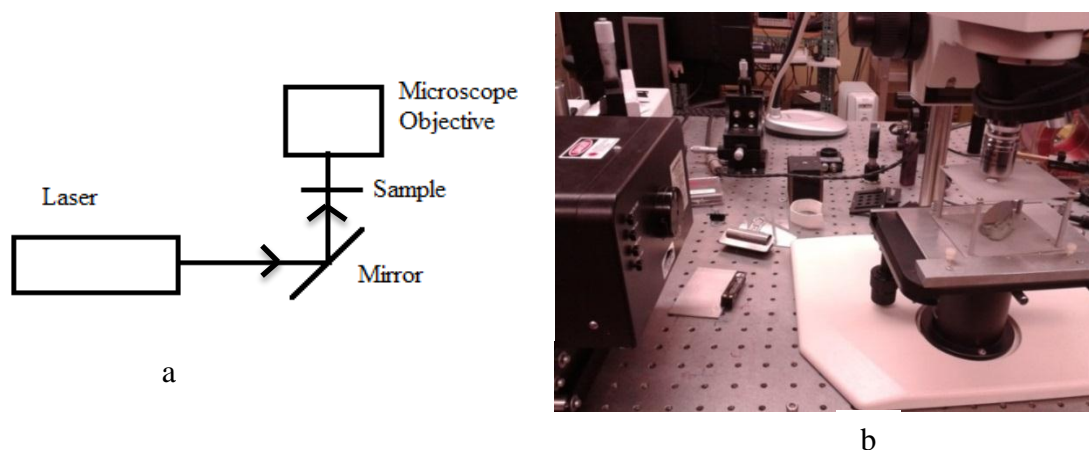


Fig. 7. Setup for image capture (a) schematics; the laser strikes the mirror and then goes through the sample into the objective (b) lab setup

For this experiment the ferrofluid is placed between two glass slides that are then pressed together so that the light would more easily transmit through the ferrofluid. Video was

then taken with the IR and visible light with no magnetic field, and then the magnetic field was applied to different axes of the sample to determine if the nanocolumns were forming. The magnetic field was supplied by the permanent magnet. To capture the images we used camera attachments to the microscope, for the 488 nm laser the Nikon DSFi-1 camera was used, and for 1550 nm laser, the FLIR Tau 320 IR camera was used.

2.3 Fourier Transform Infrared (FTIR) spectroscopy of the ferrofluid

To further explore the polarization dependence of the ferrofluid transmission as a function of magnetic field, we performed Fourier Transform Infrared (FTIR) spectroscopy measurements. FTIR spectroscopy is a technique that is used to collect a broadband IR spectrum of a sample. In FTIR, IR radiation is passed through a sample, some of the radiation is absorbed and some is transmitted through the sample. After this, an interferogram is generated in the length domain which then undergoes a Fourier Transform to generate a graph that shows the transmittance of the sample as a percentage [12]. Fig. 8 shows a block diagram of the Thermo Scientific Nexus 670 that was used in this experiment.

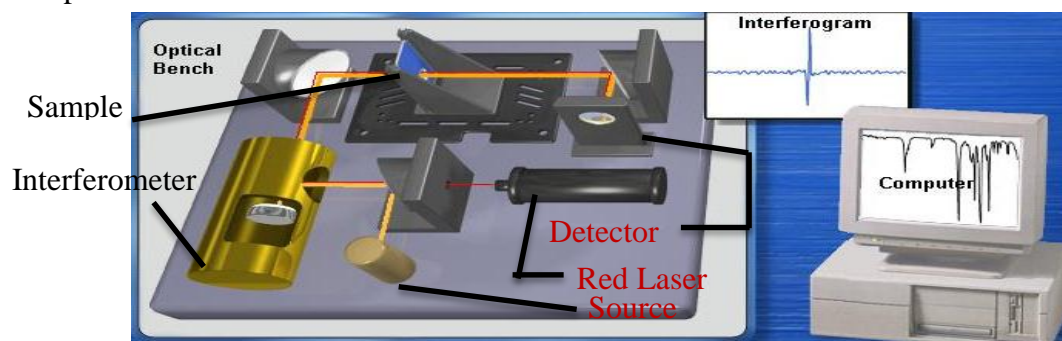


Fig. 8. Block diagram of FTIR spectrometer. The helium-neon laser is used to trigger the sampling of the interferogram, the source generates the IR radiation, which passes through a Michelson Interferometer and through the sample and to the detector. At the detector an interferogram is generated, which then undergoes a Fast Fourier Transform in the computer to generate a spectrum for the sample. [13]

Broad wavelength, $2.5\ \mu\text{m} - 16\ \mu\text{m}$, (wavenumber: $4000\ \text{cm}^{-1} - 625\ \text{cm}^{-1}$) FTIR spectroscopy was performed with and without a magnetic field applied to demonstrate the polarization dependence. The ferrofluid was put into a $200\ \mu\text{m}$ path length sample holder and the transmission measurements were measured with the polarization dependence, both with and without the magnetic field. The sample holder was two NaCl windows with a Teflon spacer, the NaCl windows were chosen because they absorb very little IR radiation. The magnetic field was created with the permanent magnet in vertical direction. Fig. 9 shows the stand and the setup that was used in the FTIR measurements, it was necessary to change out the sample holder from the spectrometer because the sample holder was magnetic and this would create a non-uniform magnetic field. An aperture was used to reduce the beam width to test a small volume of the sample, where the magnetic field could be considered uniform. A wire grid polarizer designed for long wavelength infrared (LWIR) wavelength range was placed before the sample to test the polarization dependence, and the permanent magnet was placed on a stand above the sample.

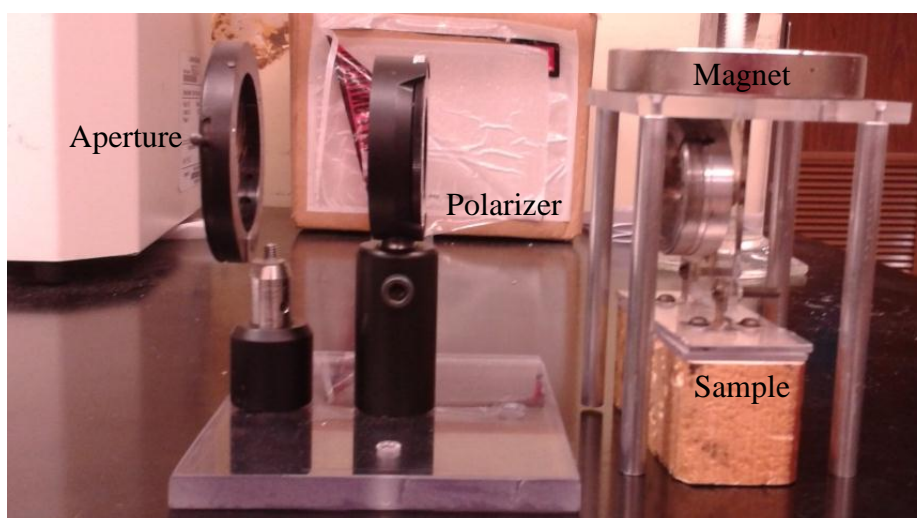


Fig. 9. Setup used inside of FTIR instead of the usual sample holder. The sample holder (wood) and magnet platform (plexiglass) are made from nonmagnetic materials.

Chapter 3

Experimental Results and Discussion

Now we show that the ferrofluid could behave as a hyperbolic metamaterial. Fig. 10 shows images from the real time observation of the ferrofluid. These images show that the ferrofluid separates into periodic regions. Depending on the magnitude of the magnetic field, the nanoparticle concentration, and the solvent used, phase separation into nanoparticle rich and nanoparticle poor regions can occur [15]. The nanoparticle rich regions appear as the black lines in Fig. 10b, while the white lines are the nanoparticle poor regions. The stripes are oriented along the direction of the applied magnetic field.

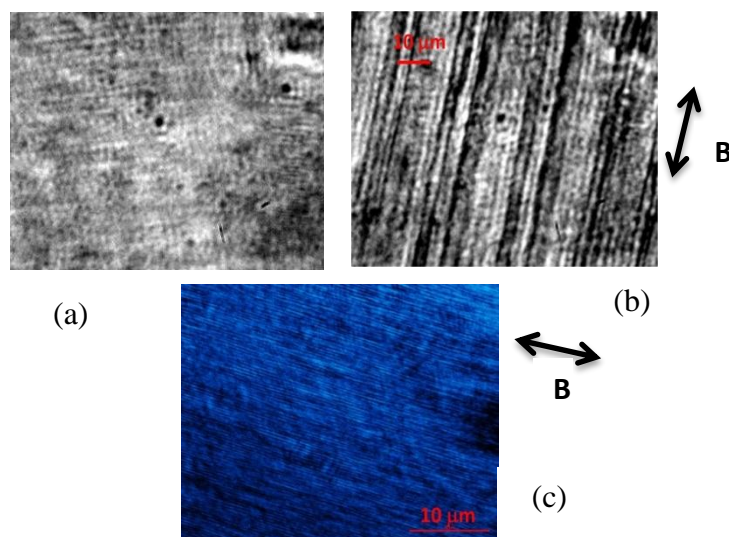


Fig. 10. Real time observation of the ferrofluid. (a) diluted ferrofluid with 1550 nm light shining through it with no magnetic field present shows random orientation (b) when the magnetic field is applied, the ferrofluid separates into nanoparticle rich and nanoparticle poor regions (c) undiluted ferrofluid with 488 nm light shows phase separation on a smaller scale. The arrows indicate magnetic field direction

3.1. Application of Maxwell-Garnett approximation to Co-based Ferrofluid

As discussed earlier, magnetic nanoparticles in a ferrofluid form nanocolumns when a magnetic field is applied. In our ferrofluid from Strem Chemicals, the average volume fraction of cobalt nanoparticles is $p = 8.2\%$. Cobalt is an excellent metal in the long wavelength infrared range (LWIR) which can be seen in Fig. 11. The real part of the refractive index, n , is much smaller than its imaginary part, k .

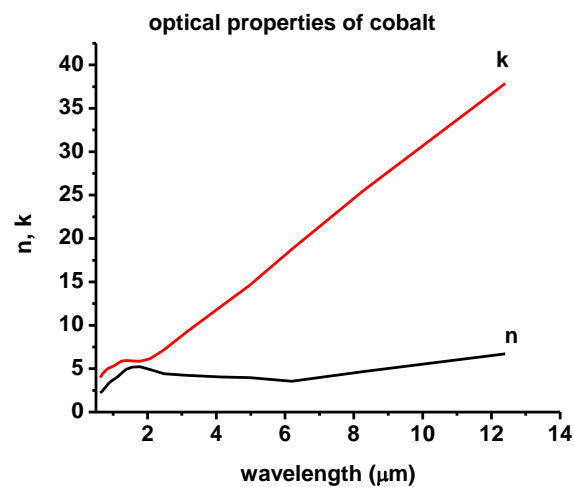


Fig. 11. Optical properties of cobalt from [14]

Because the real part is much smaller than the imaginary part, the real part, $Re(\epsilon) = n^2 - k^2$, is negative, furthermore, the absolute value is much larger than the imaginary part, $Im(\epsilon) = 2nk$. This makes the cobalt highly suitable for the fabrication of a hyperbolic metamaterial. We can again use the Maxwell-Garnett approximation to understand the electromagnetic properties of the metamaterial via the dielectric permittivities ϵ_m and ϵ_d of cobalt and kerosene, respectively. As stated earlier, the volume fraction of cobalt nanoparticles aligned into nanocolumns depends on the magnitude of the magnetic field, we will call this variable $\alpha(B)$. When the magnitude of the magnetic

field is very large, all of the nanoparticles can be assumed to be in nanocolumns so that $\alpha(\infty) = p = 8.2\%$. It can also be assumed that at smaller fields $\alpha(\infty) - \alpha(B)$ describes the cobalt nanoparticles, which are not aligned and evenly distributed in the ferrofluid. We can now use the Maxwell-Garnett approximation to determine the diagonal components of the ferrofluid permittivity.

$$\varepsilon_z = \alpha(B)\varepsilon_m + (1 - \alpha(B))\varepsilon_d \quad (8)$$

$$\varepsilon_{x,y} = \frac{2\alpha(B)\varepsilon_m\varepsilon_d + (1 - \alpha(B))\varepsilon_d(\varepsilon_d + \varepsilon_m)}{(1 - \alpha(B))(\varepsilon_d + \varepsilon_m) + 2\alpha(B)\varepsilon_d} \quad (9)$$

The calculated wavelength dependencies of ε_z and $\varepsilon_{x,y}$ at $\alpha(\infty) = p = 8.2\%$ are plotted in Fig. 12 a and b.

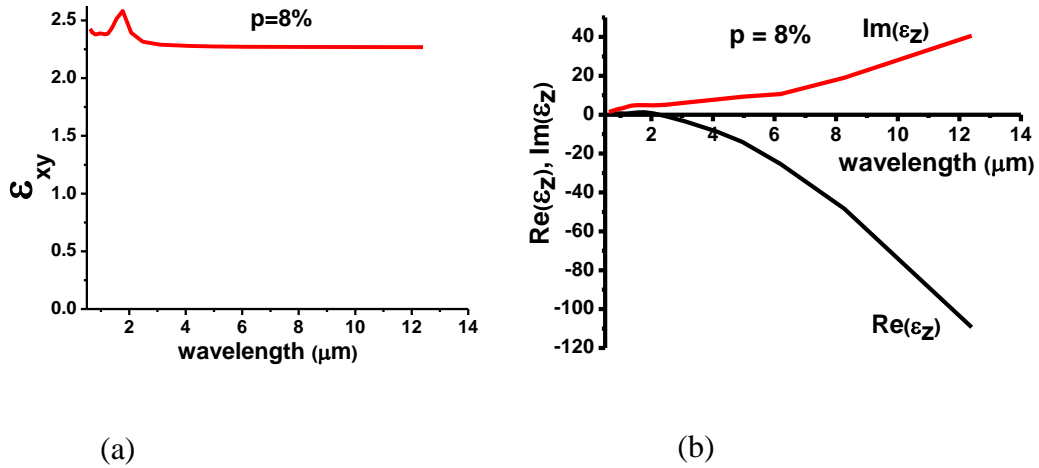


Fig. 12: (a): wavelength dependency of ε_z (b) wavelength dependency of $\varepsilon_{x,y}$

From Fig. 12 we see that $\varepsilon_{x,y}$ stays positive and nearly constant, and ε_z changes sign from positive to negative at around $\lambda = 3\mu m$. If the volume fraction of nanoparticles varies, then the sign change must occur at some critical value α_H .

$$\alpha > \alpha_H = \frac{\epsilon_d}{\epsilon_d - \epsilon_m} \quad (10)$$

α_H is plotted versus wavelength in Fig. 13, this shows that the original ferrofluid diluted with kerosene at a 1:10 ratio remains a hyperbolic medium above $\lambda = 5\mu m$.

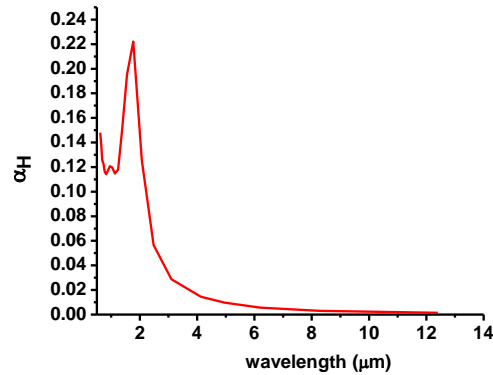


Fig. 13. α_H plotted versus free space wavelength of light, showing the transition of the ferrofluid to a hyperbolic metamaterial

The polarization dependencies of ferrofluid transmission as a function of magnetic field strength and nanoparticle concentration measured in a broad wavelength range is consistent with the hyperbolic character of ferrofluid anisotropy in the LWIR range at large enough magnetic fields. Fig. 14 shows the polarization dependent transmission spectra of a $200\mu m$ thick ferrofluid sample obtained using FTIR spectroscopy at $B = 1000G$.

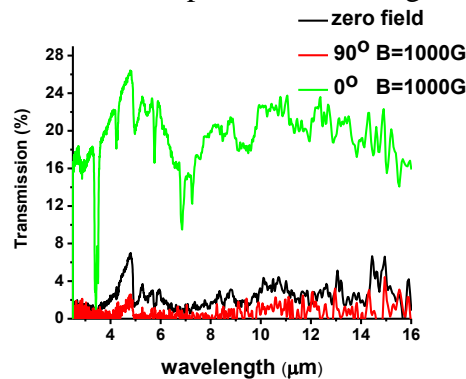


Fig. 14. FTIR spectroscopy data: transmission of $200\mu m$ ferrofluid sample for different polarization orientations and magnetic fields. The indicated angles are taken from the polarizer; 0° indicates that the E-field of light is perpendicular to the magnetic field

As seen in Fig. 14, the transmission is significantly large for the polarization direction perpendicular to the magnetic field; (electric field of the electromagnetic wave is perpendicular to the nanoparticle chains) which suggests a dielectric character of ϵ in this direction. When the polarization angle is along the nanoparticle chains, the transmission falls to near zero, which suggests a metallic character of ϵ .

If the ferrofluid can be considered a homogeneous medium, its transmission as a function of light polarization angle, φ , should behave as

$$T = T_{min}\sin^2\varphi + T_{max}\cos^2\varphi = T_{max}\left[1 - \left(\frac{T_{max}-T_{min}}{T_{max}}\right)\sin^2\varphi\right] \quad (11)$$

where T_{min} is the transmission for polarization direction parallel to the magnetic field, and T_{max} is the transmission for polarization direction perpendicular to the magnetic field. This is consistent with experimental data for visible 488 nm light (Fig. 15a) and small magnetic fields (Fig. 15b.) For larger magnetic fields the polarization dependence starts to deviate from Malus' law, which will be discussed in section 3.3.

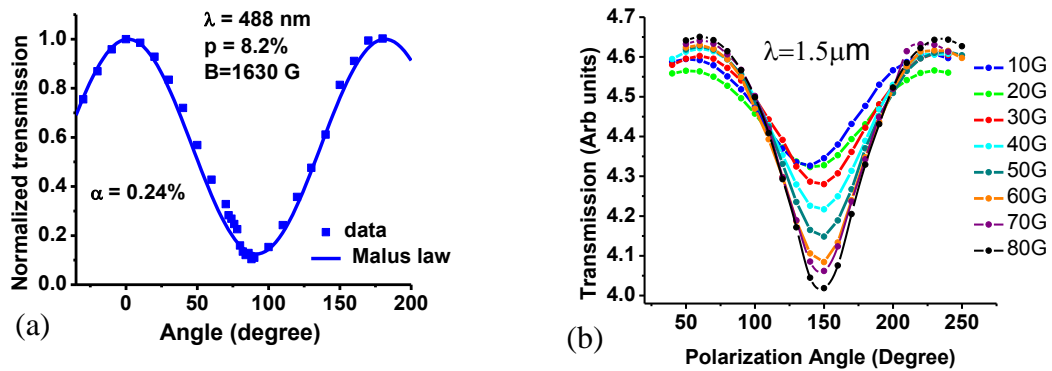


Fig. 15. Experimentally measured transmission of the cobalt based ferrofluid, $p = 8.2\%$.

(a) For visible light the polarization dependencies follow Malus' Law, showing the $\sin^2\varphi$ dependence, $B = 1630$ G. (b) The polarization dependencies show the deviation from Malus' Law at increasing magnetic fields. The lines are used as a guide to the eye.

After passing through a ferrofluid of thickness d , the electric field is given by

$$E = E_0 e^{i \frac{2\pi\sqrt{\epsilon}}{\lambda} d} \quad (12)$$

The ratio of maximum and minimum transmissions can be estimated using the expressions ϵ_z and $\epsilon_{x,y}$ from Eqn. 8 and 9.

$$\ln \left(\frac{T_{max}}{T_{min}} \right) \approx \frac{2\pi d \alpha}{\epsilon_d^{1/2}} \left(\frac{\epsilon_m''}{\lambda} \right) \quad (13)$$

This equation can be used to verify the Maxwell-Garnett Approximation and determine $\alpha(B)$. In Fig. 16, our transmission data for different wavelengths taken for identical samples in small magnetic field are consistent with the Maxwell-Garnett approximation represented by the straight line for $\alpha = 0.0004 \ll p$.

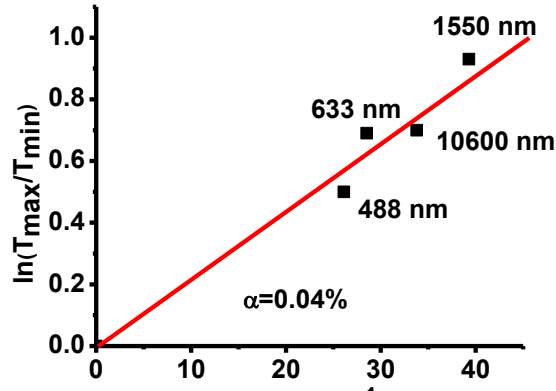


Fig. 16. Transmission data for different wavelengths. The red line represents the Maxwell Garnett approximation for $\alpha = 0.0004$ showing validity of this approximation for our sample.

It can be shown that these measurements point toward the hyperbolic character of the ferrofluid in the LWIR range. We can show this by determining $\alpha(B)$ for the polarization

curve in Fig. 15a, measured at $B = 1630$ G. The polarization contrast for this curve is

$\frac{T_{max}}{T_{min}} \approx 10$ and the curve fits Malus' Law $\sin^2\varphi$ dependence very well. From eqn. 13

$\alpha(B)$ is 0.0024 in this experiment performed at $\lambda = 488$ nm. Therefore at $\lambda = 14\mu\text{m}$, where

$Re(\epsilon_m) = -2100$, the real parts of the dielectric tensor components are given by

$$Re(\epsilon_z) \approx \alpha\epsilon'_m + \epsilon_d \approx -2.2 \text{ and } Re(\epsilon_{x,y}) \approx \epsilon_d \approx +2.1 \quad (14)$$

This means that the magnetized ferrofluid indeed exhibits hyperbolic metamaterial behavior at $\lambda = 14\mu\text{m}$.

3.2. Hyperbolic metamaterial as Minkowski spacetime analogue

From the previous description we showed that the ferrofluid has hyperbolic metamaterial behavior for LWIR. However, for $1.5\mu\text{m}$ larger concentrations of the nanoparticles are needed for ferrofluid to exhibit hyperbolic properties (Fig. 13).

Nevertheless, fluctuations of concentration could bring some regions of the sample above the hyperbolic threshold.

3.2.1. Thermal fluctuations of the nanoparticle volume fraction in ferrofluids

In principle, both ϵ_m and ϵ_d experience thermal fluctuations due to thermal fluctuations of metal and liquid densities. Density fluctuations in liquids are proportional to $(\frac{\partial V}{\partial P})_T$

[16] which is typical in an incompressible liquid far from its critical temperature.

Therefore, fluctuations of ϵ_1 and ϵ_2 must be dominated by the nanoparticle volume fraction n . If N is the number of nanoparticles in a given volume V of the ferrofluid, its standard deviation due to thermal fluctuations is given by [16]

$$\langle(\Delta N)^2\rangle = N \quad (15)$$

Therefore, the standard deviation of the nanoparticle volume fraction due to thermal fluctuations is

$$\langle(\Delta n)^2\rangle^{1/2} = \frac{n^{1/2}v^{1/2}}{V^{1/2}} \quad (16)$$

where v is the volume of an individual nanoparticle. In order for the macroscopically averaged metamaterial description to be valid, $V \gg v$. Assuming a $V > 10v$ limitation, the range of acceptable volume fluctuations is given by

$$\langle(\Delta n)^2\rangle^{1/2} \leq \frac{n^{1/2}}{3} \quad (17)$$

At this fluctuation level the metamaterial description remains valid.

The average volume fraction of our ferrofluid is $p=8.2\%$, which is below α_H for light at 1500 nm wavelength. Using eqn. 10 we can calculate the value for $\alpha_H = 17\%$ using the dielectric constants of kerosene ($\epsilon_d=1.93$) and cobalt ($Re(\epsilon_m)=-9.0$) at 1500 nm [13]. From eqn. 17 for a $(50\text{nm})^3$ of the ferrofluid; $\langle(\Delta n)^2\rangle^{1/2} = 0.04$. Therefore, at any given time, 2.3% of such volume elements should have the local value of α above α_H . Note that this 2.3% corresponds to approximately a 2σ deviation from the average nanoparticle concentration. Similarly, for a $(30\text{nm})^3$ volume of the ferrofluid gives $\langle(\Delta n)^2\rangle^{1/2} = 0.08$ so that 16% of such volume elements should have the local value of α above α_H , which corresponds to a 1σ deviation. These volume elements should exhibit transient hyperbolic behavior.

From this mathematical description it can be seen that it is possible to choose a ferrofluid that has an average $\alpha < \alpha_H$ so that, on average, this ferrofluid will be an usual elliptical material, while a considerable fraction of its volume will behave as a hyperbolic metamaterial due to the thermal fluctuations of α . The local value of α in the hyperbolic areas may temporarily exceed α_H due to thermal fluctuations. It should also be noted that the time scale of these fluctuations is much larger than the inverse light frequency at 1500 nm. Therefore, the macroscopic electrodynamics description of these areas as hyperbolic metamaterials remains valid.

3.2.2. Hyperbolic metamaterials as Minkowski spacetime analogue

Smolyaninov and Hung [18] have shown the possibility of hyperbolic metamaterials representing Minkowski spacetime. If we have a nonmagnetic uniaxial anisotropic material with dielectric permittivities $\epsilon_x = \epsilon_y = \epsilon_1$ and $\epsilon_z = \epsilon_2$; any electromagnetic field propagating through this material can be expressed as a sum of ordinary and extraordinary contributions, each being a sum of the arbitrary number of plane waves polarized in the ordinary ($E_z \equiv 0$) and extraordinary ($E_z \neq 0$) directions. We define our “scalar” extraordinary wave function $\varphi = E_z$ so that the ordinary part of the wave function does not contribute to φ . Maxwell’s Equations in the frequency domain will result in the following wave equation for φ_ω if ϵ_1 and ϵ_2 are kept constant inside the metamaterial [18].

$$\frac{\omega^2}{c^2} \varphi_\omega = -\frac{\partial^2 \varphi_\omega}{\epsilon_1 \partial z^2} - \frac{1}{\epsilon_2} \left(\frac{\partial^2 \varphi_\omega}{\partial x^2} + \frac{\partial^2 \varphi_\omega}{\partial y^2} \right) \quad (18)$$

In hyperbolic metamaterials ε_1 and ε_2 have opposite signs, so we will consider the case where $\varepsilon_1 > 0$ and $\varepsilon_2 < 0$ and we will assume that this behavior holds in some frequency range around $\omega = \omega_0$. If we assume that the metamaterial is illuminated by a coherent continuous wave (CW) laser at frequency ω_0 , and we study the spatial distribution of the extraordinary field φ_ω at this frequency. With these assumptions, Eqn. 18 can be written as:

$$-\frac{\partial^2 \varphi_\omega}{\varepsilon_1 \partial z^2} + \frac{1}{|\varepsilon_2|} \left(\frac{\partial^2 \varphi_\omega}{\partial x^2} + \frac{\partial^2 \varphi_\omega}{\partial y^2} \right) = \frac{\omega_0^2}{c^2} \varphi_\omega \quad (19)$$

which coincides with the 3D Klein-Gordon Equation (Eqn. 20) [19] describing a massive scalar field φ_ω in a 2+1 dimensional Minkowski spacetime.

$$-\frac{1}{c^2} \frac{\partial^2 \varphi}{\partial t^2} + \left(\frac{\partial^2 \varphi}{\partial x^2} + \frac{\partial^2 \varphi}{\partial y^2} \right) = \frac{m^{*2} c^2}{\hbar^2} \varphi \quad (20)$$

Note that the spatial coordinate $z = t$ behaves as a timelike variable in Eqn. 19.

On average, the ferrofluid metamaterial is an elliptical material, but the thermal fluctuations of the nanoparticle concentration lead to the transient formation of hyperbolic regions inside the metamaterial. These regions behave as transient 2+1 dimensional Minkowski Spacetimes which temporarily appear and disappear inside the larger metamaterial “multiverse”

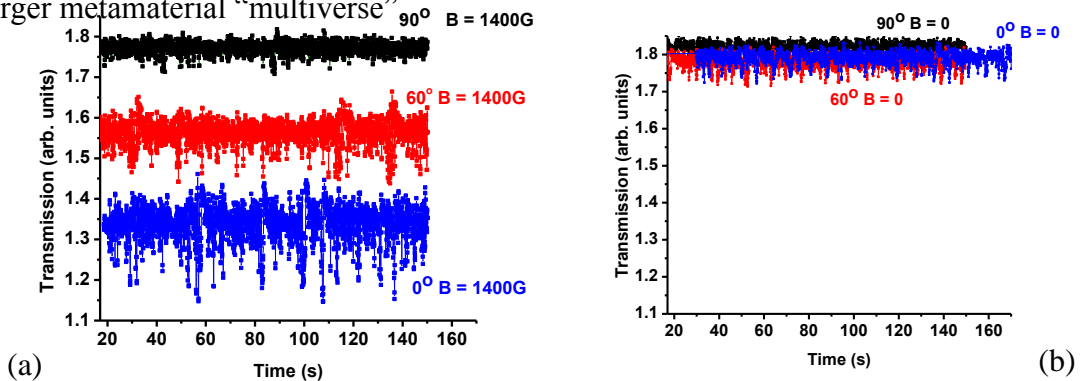


Fig. 17. Experimentally observed temporal fluctuations of the sample transmission at 1550 nm (a) in magnetic field of 1400 G; (b) in zero magnetic field. The angles indicated are taken from the polarizer; 0° indicates that the E-field of light is perpendicular to the magnetic field

Figure 17 shows measured temporal fluctuations of the sample transmission, which exhibit strong dependence on the polarization states of the incident light, when magnetic field is applied. The fluctuations are strongest when the E-field of the incident light is direct along the external magnetic field. Short bursts of increased fluctuations are also seen, this can be explained by the nanocolumns suddenly breaking down and rearranging. In Fig.18 we compare different concentrations of cobalt nanoparticles. At much lower concentrations the polarization dependence of the transmission fluctuations disappears. The figure demonstrates that the observed effect disappears far from the hyperbolic edge.

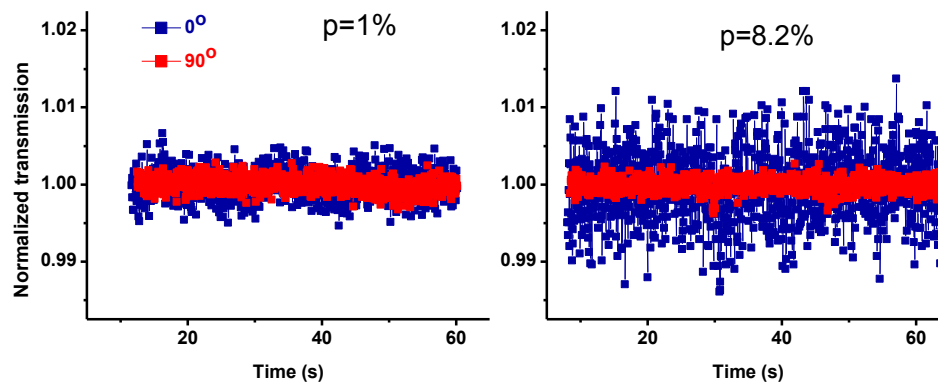


Fig. 18. Fluctuations for different nanoparticle concentrations.

3.3 Polarization “notch”

Based on the Maxwell-Garnett Approximation, at small magnetic fields where $\alpha(B) \ll p$ we obtain

$$\varepsilon_z = \alpha\varepsilon_m + (1 - \alpha)\varepsilon_d \approx \varepsilon_d + i\alpha\varepsilon_m'' \text{ and } \varepsilon_{x,y} \approx \varepsilon_d \quad (21)$$

where ε_m'' is the imaginary part of ε_m . Fig. 15b and 19 show the transmission of the IR laser through the ferrofluid with different values for the magnetic field B. When the magnetic field is zero the transmission is isotropic (weak polarization dependence is possibly due to residual alignment of the nanoparticles in remnant magnetic field). However, as the magnetic field is increased the transmission becomes highly anisotropic. At smaller values of magnetic fields the polarization dependencies follow Malus' Law, showing the $\sin^2\varphi$ dependence. For larger magnetic fields the polarization dependence starts to deviate from Malus' law (Fig. 15b and 19.) The IR transmission has pronounced minima (notches) when E-field of the wave is parallel to the direction of the external magnetic field.

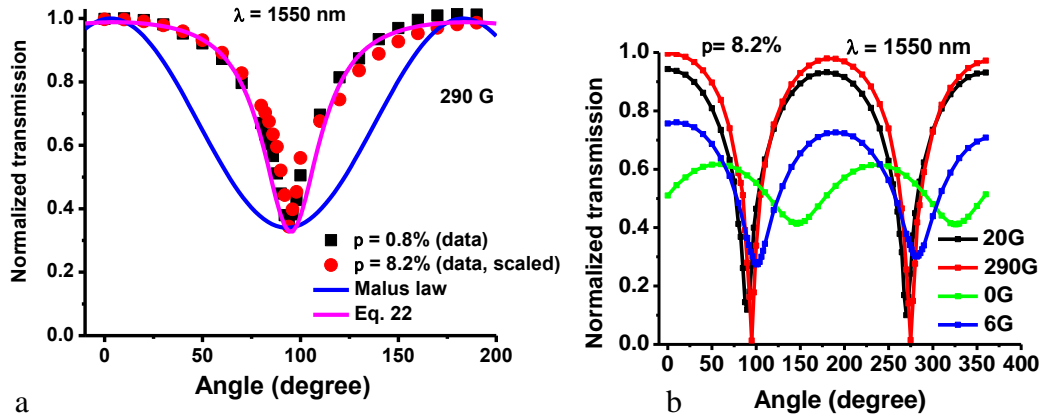


Fig. 19. Polarization and magnetic field dependence of ferrofluid transmission for 1550 nm wavelengths: (a) data for different concentrations of nanoparticles in the ferrofluid can be fitted to Eq. 22 (pink line), which significantly differs from Malus' law (blue line); (b) sharp decrease of transmission near extinction angle, "polarization notch," at increasing magnetic fields

The polarization dependencies of the ferrofluid measured at different nanoparticle concentrations (Fig. 19a) can be fitted to a "polarization notch" described empirically by

$$T \sim \frac{1 - a \sin^2 \theta}{1 + b \cos^2 \theta} \quad (22)$$

This “polarization notch” dependence may arise from the multiple scattering of light by periodically spaced nanoparticle rich and nanoparticle poor phases forming a Fabry-Perot-like resonator. The transmission amplitude, t , through such a resonator is given by a sum of all of the multiple scattering events in which the wave experiences multiple polarization dependent reflections from the phase boundaries

$$t = \sum_{m=0}^{\infty} t_m = t_0 \sum_{m=0}^{\infty} r^m e^{im\delta} = \frac{t}{1 - r e^{i\delta}} \quad (23)$$

where δ is the phase accumulated by the wave when it passes through both phase boundaries. The resulting transmission through a single resonator formed by the nanoparticle rich and poor phases is given by

$$T = t t^* = \frac{t^2}{1 + r^2 - 2r \cos \delta} \quad (24)$$

Because both t and r exhibit strong polarization dependencies, the polarization notch description (Eqn. 22) can be explained.

3.4 FTIR spectroscopy

Broadband divergence of the photonic density of states in hyperbolic metamaterials significantly modifies radiative decay rates radiation lifetime [4, 6]. This is another useful check to determine if our ferrofluid is indeed acting as a hyperbolic metamaterial; the absorption lines of kerosene can be used to test this effect. The absorption spectra measured with FTIR spectrometer with and without magnetic field (Fig/ 20) are consistent with the decrease in the radiation lifetime of kerosene molecules in the

hyperbolic state. This shorter lifetime leads to a decrease in absorption line amplitude and is seen in Fig. 20.

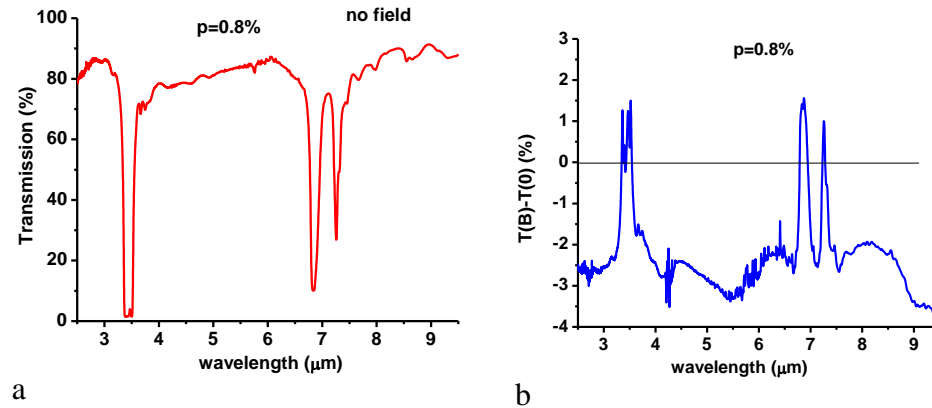


Fig. 20. FTIR transmission of the diluted ferrofluid. (a) zero magnetic field demonstrates kerosene absorption lines; (b) differential FTIR spectrum shows decrease in absorption line amplitude, which is consistent with the decrease of the kerosene radiation lifetime in the hyperbolic metamaterial state.

It has also been reported by Narimanov et al, that reduced reflection is another experimental indicator of hyperbolic metamaterials [6]. Due to broadband divergence of photonic density of states, roughened surface of a hyperbolic metamaterial scatters light preferentially inside the medium, resulting in reduced reflectance. This can also be checked with our spectra; Fig. 21 a and b show that our sample does indeed show reduced reflectance and is another indicator that our cobalt based ferrofluid is acting as a hyperbolic metamaterial.

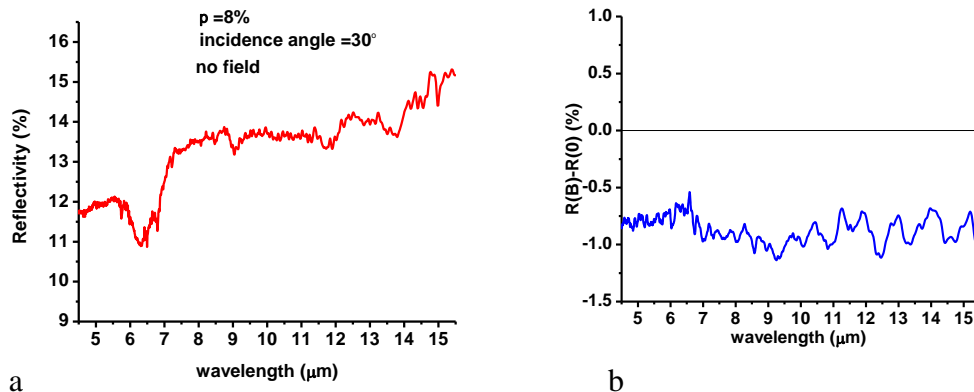


Fig. 21. FTIR reflection of the non-diluted ferrofluid gives another indication that the ferrofluid is acting as a hyperbolic metamaterial. (a) zero magnetic field; (b) differential FTIR reflection spectrum demonstrates the reduced reflectivity of the ferrofluid in magnetic field.

Chapter 4

Conclusions

We have studied the optical properties of a cobalt based ferrofluid. In the study we have performed experiments including the transmission of light through the sample and FTIR spectroscopy. The ferrofluid was studied with and without the presence of an external magnetic field. Cobalt nanoparticles in ferrofluid are self-assembled into nanocolumns in a magnetic field. There are nanocolumn rich and nanocolumn poor regions, which are arranged as stripes in the magnetic field.

The validity of application of Maxwell-Garnet approximation to this ferrofluid was confirmed. Calculations performed using Maxwell-Garnet approximation and optical parameters of cobalt and kerosene showed that the ferrofluid in magnetic field has the dispersion relation of hyperbolic metamaterial for LWIR range. Polarization dependence of transmission data for a broad wavelength range is consistent with hyperbolic behavior;

light polarized in the direction along the columns propagates poorly, as in metallic media, but light polarized in the direction perpendicular to the columns propagates as through a dielectric.

From FTIR spectroscopy measurements we have found reduction of the kerosene absorption line amplitude and reduction of the reflectance of the ferrofluid in magnetic field. These results confirm hyperbolic character of the ferrofluid in the LWIR range, where large optical density of states leads to a reduction in the radiation lifetime. Our experiments and analysis have shown conclusively that the cobalt-based ferrofluid sample is a hyperbolic metamaterial.

As a hyperbolic material, ferrofluid is an optical analog of Minkowski spacetime. We have experimentally transient formation of hyperbolic regions in a ferrofluid below the hyperbolic threshold, which is an analogue to transient 2+1 dimensional Minkowski spacetime regions.

We have found a sharp reduction of transmission near extinction angle for a ferrofluid in magnetic field, a “polarization notch,” a deviation from Malus’ law not observed previously. This behavior can be explained by multiple reflections from nanocolumn-rich regions.

While traditional metamaterials require complex nanofabrication and therefore have limited dimensions, a ferrofluid is truly three-dimensional metamaterial, which is easy to produce. Studied properties of ferrofluid as hyperbolic metamaterial indicate potential applications in chemical and biological sensing.

Bibliography

- [1] R.A. Shelby, D.R. Smith, S.C. Nemat-Nasser, S. Schultz, “Microwave Transmission Through a Two-Dimensional, Isotropic, Left-Handed Metamaterial”, *Appl. Phys. Lett.* **78**, 489 (2001).
- [2] C. Kittel, *Introduction to Solid State Physics* (Wiley & Sons, 2004). Vol. 8.
- [3] P. Shekhar, J. Atkinson, Z. Jacob, “Hyperbolic Metamaterials: Fundamentals and Applications”, Arxiv 1401.2453.
- [4] J. Kim, V.P. Drachev, Z. Jacob, G.V. Naik, A. Boltasseva, E.E. Narimanov, V.M Shalaev, “Improving the Radiative Decay Rate for Dye Molecules with Hyperbolic Metamaterials”, *Optics Express* **20**, 8100 (2012).
- [5] T.U. Tumkur, L. Gu, J.K. Kitur, E.E. Narimanov, M.A. Noginov, “Control of Absorption with Hyperbolic Metamaterials”, *Appl. Phys. Lett.* **100**, 161103 (2012).
- [6] E.E. Narimanov, H. Li, Yu. A. Barnakov, T.U. Tumkur, M.A. Noginov, “Reduced Reflection from Roughened Hyperbolic Metamaterial”, *Optics Express* **21**, 14956 (2013).
- [7] H. Zhang, M. Widom, “Spontaneous Magnetic Order in Strongly Coupled Ferrofluids”, *J. of Magnetism and Magnetic Mat.* **122**, 119 (1993).
- [8] Y. Gao, J.P. Huang, Y.M. Liu, L. Gao, K.W. Yu, X. Zhang, “Optical Negative Refraction in Ferrofluids with Magnetocontrollability”, *Phys. Rev. Lett.* **104**, 034501 (2010).

- [9] K. Butter, P.H.H Bomans, P.M. Frederik, G.J. Vroege, A.P. Philipse, “Direct Observation of Dipolar Chains in Iron Ferrofluids by Cryogenic Electron Microscopy”, *Nature Mat.* **2**, 88 (2003).
- [10] W. Cai, V. Shalaev, *Optical Metamaterials Fundamentals and Applications*, (Springer, 2010) Vol. 1.
- [11] R. Wangberg, J. Elser, E.E. Narimanov, V.A. Podolskiy, “Nonmagnetic Nanocomposites for Optical and Infrared Negative-Refractive-Index Media”, *J. Opt. Soc. Am. B* **23**, 498 (2006).
- [12] J.M. Hollas *Modern Spectroscopy* (Wiley & Sons, 2004). Vol. 4.
- [13] Thermo Scientific, *Guide to FT-IR*.
- [14] *CRC Handbook of Chemistry and Physics*, (CRC Press, 2005).
- [15] A.J. Hoffman, L. Alekseyev, S.S. Howard, K.J. Franz, D. Wasserman, V.A. Podolskiy, E.E. Narimanov, D.L. Sivco, C. Gmachl, “Negative Refraction in Semiconductor Metamaterials”, *Nature Mat.* **6**, 946 (2007).
- [16] L.D. Landau, E.M. Lifshitz, L.P. Pitaevskii, *Course of Theoretical Physics* (Reed, 1984). Vol. 5.
- [17] I.I. Smolyaninov, E.E. Narimanov, “Metric Signature Transitions in Optical Metamaterials”, *Phys. Rev. Lett.* **105**, 067402 (2010).
- [18] I.I. Smolyaninov, Y.J. Hung, “Modeling of Time with Metamaterials”, *J. Opt. Soc. Am. B* **28**, 1591 (2011).

- [19] J.J. Sakurai, *Advanced Quantum Mechanics*. (Addison Wesley 1967)
- [20] I.I. Smolyaninov, B. Yost, E. Bates, V.N. Smolyaninova, “Experimental Demonstration of Metamaterial Multiverse in a Ferrofluid”, *Optics Express* **21**, 14918 (2013).
- [21] V.N. Smolyaninova, B. Yost, D. Lahneman. E.E. Narimanov, I.I. Smolyaninov, “Self-Assembled Tunable Photonic Hyper-Crystals”, unpublished, Arxiv 1312.7138.

Curriculum Vita

Bradley J. Yost

██

██

Applied Physics

Master of Science, 2014

Fort Hill High School, Cumberland, MD 2002

Towson University	2012-2014	Master of Science	2014
-------------------	-----------	-------------------	------

Major: Applied Physics

Towson University	2012-2013	Post Baccalaureate Certificate	2013
-------------------	-----------	--------------------------------	------

Major: Program, Portfolio, and Project Management

Frostburg State University	2010-2012	Bachelor of Science	2012
----------------------------	-----------	---------------------	------

Major: Applied Physics

Minor: Mathematics

Allegheny College of Maryland	2009-2010	Associate of Science	2010
-------------------------------	-----------	----------------------	------

Major: Physics

Professional Publications:

V.N. Smolyaninova, B. Yost, D. Lahneman, E.E. Narimanov, I.I. Smolyaninov, “Self-Assembled Tunable Photonic Hyper-Crystals” Arxiv: 1312.7138; Under consideration: Scientific Reports

I.I. Smolyaninov, B. Yost, E. Bates, V.N. Smolyaninova, “Experimental Demonstration of Metamaterial Multiverse in a Ferrofluid” Optics Express 21, 14918-14925 (2013) This work generated considerable media interest including MIT Technology Review, ExtremeTech, The Economist, etc.

Professional Presentations:

B. Yost, D. Lahneman, V. N. Smolyaninova, “Reconfigurable tunable hyperbolic metamaterial” TU Undergraduate and Graduate Student Research and Performance Expo, 2013

B. Yost, D. Lahneman, E. Bates, V.N. Smolyaninova, I.I. Smolyaninov, “Selfassembled Metamaterials: Minkowski Spacetime Analogue”, APS March Meeting 2014.

E. Bates, B. Yost, I. I. Smolyaninov, V. N. Smolyaninova, "Ferrofluids as hyperbolic metamaterials," the 2013 Colonial Academic Alliance Undergraduate Research Conference, Newark, DE

B. Yost, E. Bates, I. I. Smolyaninov, V. N. Smolyaninova, "Ferrofluids as hyperbolic metamaterials," the Morgan State 20th Annual Undergraduate & Graduate Science Research Symposium

B. Yost, E. Bates, I. I. Smolyaninov V. N. Smolyaninova, "Ferrofluids as hyperbolic metamaterials" TU Undergraduate and Graduate Student Research and Performance Expo, 2013

I. I. Smolyaninov, B. Yost, E. Bates, and V.N. Smolyaninova, "Experimental demonstration of metamaterial "multiverse" in a ferrofluid," SPIE 2013, San Diego, CA, invited talk.

D. Lahneman, B. Yost, V. Smolyaninova "Magnetic Ferrofluids as Hyperbolic Metamaterials" National Conference NCUR14, University of Kentucky

Professional Positions Held:

Laboratory Research Assistant

Towson University, Towson MD, 21252

